

Search for Quadrupole Strength in the Electro-excitation of the $\Delta^+(1232)$

C. Mertz,^{1,2} C. Vellidis,² R. Alarcon,¹ D.H. Barkhuff,³ A.M. Bernstein,⁴ W. Bertozzi,⁴ V. Burkert,⁵ J. Chen,⁴ J.R. Comfort,¹ G. Dodson,⁴ S. Dolfini,¹ K. Dow,⁴ M. Farkhondeh,⁴ J.M. Finn,⁶ S. Gilad,⁴ R.W. Gothe,⁷ X. Jiang,⁸ K. Joo,⁴ N.I. Kaloskakis,^{2,4} A. Karabarounis,² J.J. Kelly,⁹ S. Kowalski,⁴ C. Kunz,⁷ R.W. Lourie,³ J.I. McIntyre,⁶ B.D. Milbrath,³ R. Miskimen,⁸ J.H. Mitchell,⁵ C.N. Papanicolas,² C.F. Perdrisat,⁶ A.J. Sarty,¹⁰ J. Shaw,⁸ S.-B. Soong,⁴ D. Tieger,⁴ C. Tschalær,⁴ W. Turchinets,⁴ P.E. Ulmer,¹¹ S. Van Verst,⁴ G.A. Warren,⁴ L.B. Weinstein,¹¹ S. Williamson,¹² R.J. Woo,⁶ A. Young¹

¹*Department of Physics and Astronomy, Arizona State University, Tempe, Arizona 85287*

²*Institute of Accelerating Systems and Applications and Department of Physics, University of Athens, Athens, Greece*

³*Institute for Nuclear and Particle Physics and Department of Physics, University of Virginia, Charlottesville, Virginia 22901*

⁴*Department of Physics, Laboratory for Nuclear Science and Bates Accelerator Center, Massachusetts Institute of Technology, Cambridge, Massachusetts 02139*

⁵*Thomas Jefferson National Accelerator Facility, Newport News, Virginia 23606*

⁶*Physics Department, College of William and Mary, Williamsburg, Virginia 23187*

⁷*Department of Physics, Bonn University, Bonn, Germany*

⁸*Department of Physics, University of Massachusetts, Amherst, Massachusetts 01003*

⁹*Department of Physics, University of Maryland, College Park, Maryland 20742*

¹⁰*Department of Physics, Florida State University, Tallahassee, Florida 32306*

¹¹*Department of Physics, Old Dominion University, Norfolk, Virginia 23529*

¹²*Physics Department, University of Illinois, Urbana-Champaign, Illinois 61801*

(November 21, 2021)

High-precision $H(e, e'p)\pi^0$ measurements at $Q^2 = 0.126$ (GeV/c)² are reported, which allow the determination of quadrupole amplitudes in the $\gamma^*N \rightarrow \Delta$ transition; they simultaneously test the reliability of electroproduction models. The derived quadrupole-to-dipole amplitude ratios, $R_{SM} = (-6.5 \pm 0.2_{\text{stat+sys}} \pm 2.5_{\text{mod}})\%$ and $R_{EM} = (-2.1 \pm 0.2_{\text{stat+sys}} \pm 2.0_{\text{mod}})\%$, are dominated by model error. Previous R_{SM} and R_{EM} results should be reconsidered after the model uncertainties associated with the method of their extraction are taken into account.

13.60.Le,14.20.Gk,25.30.Rw

The conjecture that the nucleon is deformed, raised more than 20 years ago [1], continues to be the subject of intense theoretical [2–8] and experimental [9–15] activity. Because the quadrupole moment of the nucleon vanishes on account of its spin-1/2 nature, this investigation has naturally turned to the search for quadrupole strength in the $\gamma^*N \rightarrow \Delta(1232)$ transition.

Spin-parity selection rules in the $N(J^\pi = 1/2^+) \rightarrow \Delta(J^\pi = 3/2^+)$ transition allow magnetic dipole (M1) and electric (E2) or Coulomb quadrupole (C2) amplitudes. In the naive (spherical) quark model of the nucleon, the Δ excitation is understood as a pure spin-flip (M1) transition. Experimentally, M1 is indeed found to dominate. In more refined models, small E2 and C2 amplitudes are predicted. The physical origin of these contributions is attributed to different mechanisms in the various models. However they invariably have important implications for our understanding of the structure of the nucleon and of QCD at low energies [2–5].

In pion production, the multipole amplitudes are denoted by $M_{l\pm}^I$, $E_{l\pm}^I$, and $S_{l\pm}^I$, indicating their character (magnetic, electric, or scalar), their isospin (I), and their total angular momentum ($J = l \pm 1/2$). Thus, the resonant photon multipoles M1, E2, and C2 correspond to $M_{1+}^{3/2}$, $E_{1+}^{3/2}$, and $S_{1+}^{3/2}$, respectively. The Electric and Scalar-to-Magnetic-Amplitude-Ratio are defined as $R_{EM} = \Re(eE_{1+}^{3/2}/M_{1+}^{3/2})$ and $R_{SM} = \Re(S_{1+}^{3/2}/M_{1+}^{3/2})$ respectively. Most models of the nucleon have definite predictions for these ratios. They are invariably very small at low momentum transfers, the domain of the reported measurements. The predictions for R_{EM} at $Q^2 = 0$ range from -0.1% up to -5% [2–5].

While R_{EM} measurements at $Q^2 = 0$ are pursued with the use of real photons, its Q^2 evolution and the R_{SM} ratio can be investigated only through electro-excitation. A number of calculations explore the dependence of R_{EM} and R_{SM} on Q^2 [2,6–8]. The experimental determination of R_{EM} and R_{SM} is severely complicated by the presence of non-resonant processes that are coherent with the resonant excitation of the $\Delta(1232)$ [16]. These processes (such as Born contributions and tails of higher resonances), termed “background contributions,” need to be constrained with model calculations and measurements tailored to this end. Also, it is imperative that electro-production models, used in model extraction of R_{EM} and R_{SM} , are adequately tested in their ability to accurately handle small amplitudes, both resonant and background.

Precision measurements with polarized tagged photons have resulted in an R_{EM} at resonance of $(-3.0 \pm 0.3)\%$ [9] and $(-2.5 \pm 0.3)\%$ [10]. Model calculations are in reasonably good agreement with experiment [17–19]. The situation is quite different for electron scattering investigations. Experiments conducted in the late 60’s and early 70’s for Q^2 up to 1 (GeV/c)² have yielded R_{EM} values consistent with zero and R_{SM} of around -7% with large statistical and systematic errors [11–13]. A dispersion relation analysis [20] reported exceptionally large values

of R_{SM} around -13% in the range of $Q^2 = 0.1 - 0.25$ (GeV/c)², suggestive of a narrow structure peaking near $Q^2 = 0.1$ (GeV/c)². These values are consistent with the value $\Re(eS_{1+}/M_{1+}) = (-12.7 \pm 1.5)\%$ of the ratio of isospin-mixed multipoles which was reported in a recent $H(e, e'\pi^0)p$ experiment at $Q^2 = 0.127$ (GeV/c)² [14]. The measurements reported here, performed at the same Q^2 , allow a direct comparison with the afore-mentioned data.

The coincident $H(e, e'\pi^0)$ cross section in the One-Photon-Exchange-Approximation can be written as [21]:

$$\frac{d\sigma}{d\omega d\Omega_e d\Omega_{pq}^{cm}} = \Gamma_v \frac{p_{cm}}{k_{cm}} \sigma, \quad (1)$$

$$\sigma = R_T + \varepsilon_L R_L - \rho_{LT} R_{LT} \cos \phi + \varepsilon R_{TT} \cos 2\phi,$$

where Γ_v is the virtual photon flux; p_{cm} and k_{cm} are the pion momentum and the photon equivalent energy in the hadronic CM frame, respectively; ε , ε_L , and ρ_{LT} are electron kinematic factors; and ϕ is the nucleon azimuthal angle about the momentum transfer \vec{q} measured from the nucleon direction closest to the beam exit line. R_L , R_T , R_{LT} , and R_{TT} are the longitudinal, transverse, longitudinal-transverse, and transverse-transverse interference response functions, respectively [21].

To study the $\gamma^*N \rightarrow \Delta$ transition with high precision, an extensive program has been developed at the MIT-Bates Linear Accelerator. We report here results from the first phase of the program. We have reported the recoil proton polarization P_n result from the same experiment [22].

The experiment [22,23] was conducted at energies of 719 and 799 MeV and a liquid H₂ target was used; the scattered electrons were detected in the “MEPS” spectrometer and the coincident protons in “OHIPS”. The focal plane instrumentation of each spectrometer consisted of one crossed vertical drift chamber for track reconstruction and scintillators for triggering. Detailed optics studies were done for each spectrometer, and the detection efficiencies were measured as functions of all independent reaction coordinates. The phase-space normalization of the cross section and various corrections applied to the data, including radiative corrections, were implemented with the aid of a Monte Carlo simulation model. The coincident cross section was measured at $\phi = 0$ and π for a broad range of hadronic mass W around the resonance and a range of proton polar angle θ about \vec{q} in the hadronic CM frame near $\theta = 0$.

Fig. 1 shows the coincident cross section as a function of the hadronic mass W for proton detection at $\theta = 0$, where R_{LT} and R_{TT} vanish and R_T has the maximum sensitivity to $\Re(eE_{1+}^*M_{1+})$. The data exhibit a distinct resonant shape, arising mostly from $|M_{1+}|^2$. Fig. 2 shows the response function R_{LT} and the cross section asymmetry A_{LT} which are sensitive to $\Re(S_{1+}^*M_{1+})$,

$$A_{LT} = \frac{\sigma_{\phi=0} - \sigma_{\phi=\pi}}{\sigma_{\phi=0} + \sigma_{\phi=\pi}} = \frac{-\rho_{LT} R_{LT}}{R_T + \varepsilon_L R_L + \varepsilon R_{TT}}. \quad (2)$$

The measured cross section (Fig. 1), asymmetry and R_{LT} response function (Fig. 2), are compared with the curves that result by adjusting the relevant parameters in the models of Drechsel *et al.* [17,24] (MAID), of Sato and Lee (SL) [18,25], and of Davidson and Mukhopadhyay (RPI) [19,26]. All three models start from the same Lagrangian for the non-resonant terms, including explicit nucleon and light meson (π , ρ , ω) degrees of freedom coupled to the electromagnetic field. Their principal differences lie in the definition of the Δ resonance and in the method of unitarization. The solid curve is the fit of the MAID-2000 code, where the five parameters controlling the electromagnetic couplings of the $\Delta(1232)$ and of the $P_{11}(1440)$ (Roper) resonances were fitted to our data. The long-dashed curve results by adjusting all seven free parameters of the RPI model, in a fashion similar to that reported in [15], while the short-dashed curve results by judiciously adjusting (without χ^2 minimization) the parameters of the SL model to the data. All calculations properly obtain the position of the cross section maximum. They differ in their detailed shape and in magnitude. The adjusted MAID-2000 and RPI models provide an excellent description of the data, with the possible exception of the high W points.

The A_{LT} and R_{LT} results (Fig. 2) amply demonstrate the sensitivity of our data to the presence of resonant quadrupole amplitudes. All three models fail dramatically if the resonant quadrupole amplitudes are set to zero. However, when the quadrupole strength is adjusted, good agreement is achieved.

The sensitivity of our data to the quadrupole amplitudes allows for the determination of R_{EM} and R_{SM} either through a variant of the M1-dominance truncated multipole expansion (“TME”) fit (as in [11–14]) or through model extraction, as in [15]. The derived values are shown in Table I. In TME fit (a), as in [14], it is assumed that only the multipoles M_{1+} and S_{1+} contribute and that R_L is insignificant. Then we obtain $\Re e(S_{1+}/M_{1+}) = (-7.6 \pm 0.3_{\text{stat}} \pm 0.7_{\text{sys}})\%$. The hatched band in Fig. 2 shows the projected asymmetry (1σ confidence) for our angular range if the Bonn $\Re e(S_{1+}/M_{1+}) = (-12.7 \pm 1.5_{\text{stat}})\%$ [14] is adopted. Our data points lie several standard deviations away. Noting that A_{LT} was measured in [14] near $\theta = 180^\circ$, the discrepancy may indicate that terms having a different dependence on θ than those included in TME fit (a) contribute significantly. If all three 1^+ multipoles are adjusted, setting $|S_{1+}|^2 = |E_{1+}|^2 = \Re e(S_{1+}^* E_{1+}) = 0$, the derived value of $\Re e(S_{1+}/M_{1+})$, labeled with “TME (b)” in Table I, is noticeably larger, although not incompatible with, the value extracted through TME fit (a). This is a manifestation of the significant truncation error that characterizes the TME approach.

$\Re e(S_{1+}/M_{1+})$ and $\Re e(E_{1+}/M_{1+})$ values are also obtained from the fits of the MAID-2000 [24] and RPI [26] models and from the adjustment of the SL model [25]. While all three models achieve a reasonable agreement with the unpolarized data (Figs. 1 and 2), the result-

ing values of P_n disagree with each other (Table I) and with the experimental value $P_n = -0.397 \pm 0.055_{\text{stat}} \pm 0.009_{\text{sys}}$ [22]. The MAID-2000 value could be considered as providing a fair agreement, lying within two standard deviations from the experimental value.

Given the overall success of the MAID-2000 model fit in accounting for our data, we adopt the values $R_{SM} = (-6.5 \pm 0.2_{\text{stat+sys}})\%$, $R_{EM} = (-2.1 \pm 0.2_{\text{stat+sys}})\%$, and $|M_{1+}^{3/2}| = (39.8 \pm 0.3_{\text{stat+sys}}) \times 10^{-3}/m_{\pi^+}$. The statistically incompatible values provided by the other two, equally sophisticated, model analyses indicate that the results are characterized by substantial model uncertainty. The quantification of this uncertainty for each one of the available models is urgently needed. It could remove the apparent contradictions among the available models. We assume that the scatter of the extracted values provides an estimate of the model uncertainty. We therefore attribute, conservatively, to R_{SM} and R_{EM} model uncertainties of $\pm 2.5\%$ and $\pm 2.0\%$ respectively, and to $|M_{1+}^{3/2}|$ a model uncertainty of $\pm 2.0 \times 10^{-3}/m_{\pi^+}$. Previously published R_{SM} and R_{EM} results [11–15] have not taken into account this uncertainty. They are subject to comparable model error. This added uncertainty may remove all known inconsistencies amongst them, when properly estimated.

The data presented here exhibit unprecedented sensitivity to the presence of resonant quadrupole amplitudes. Their analysis leads us to the following conclusions: i) Extractions of quadrupole strengths based on TME fits are characterized by substantial truncation error and lead to inconsistent results; ii) Claims of large R_{SM} at low Q^2 derived from earlier [20] and recent [14] measurements cannot be supported; iii) Even when conservative estimates of systematic and model uncertainties are taken into consideration, an unambiguously negative value for R_{SM} is obtained. This value supports the claims for an oblate deformed Δ ; and iv) The available pertinent electroproduction models are on the verge of successfully describing the high precision data that are now emerging. It is important that the model errors due to input parameters and model assumptions be quantified. It is essential that measurements be performed that are sensitive to background amplitudes, along with those that are primarily sensitive to quadrupole amplitudes.

We are indebted to Drs. S.S. Kamalov, D. Drechsel, L. Tiator, R.M. Davidson, N.C. Mukhopadhyay, T.-S.H. Lee, T. Sato, and J.M. Laget for providing us with detailed calculations and valuable comments concerning their models and the issue of “nucleon deformation.”

-
- [1] S. L. Glashow, *Physica* **96A**, 27 (1979).
 - [2] S. Capstick and G. Karl, *Phys. Rev.* **D41**, 2767 (1990);
S. Capstick and B. D. Keister, *Phys. Rev.* **D51**, 3598

(1995).

- [3] G. K. N. Isgur *et al.*, Phys. Rev. **D25**, 2394 (1982).
- [4] C. E. Carlson, Phys. Rev. **D34**, 2704 (1986).
- [5] A. J. Buchmann *et al.*, Phys. Rev. **C55**, 448 (1997).
- [6] D. H. Lu *et al.*, Phys. Lett. **C55**, 3108 (1997).
- [7] S. S. Kamalov and S. N. Yang, Phys. Rev. Lett **83**, 4494 (1999).
- [8] G. C. Gellas *et al.*, Phys. Rev. **D60**, 54022 (1999).
- [9] G. Blanpied *et al.*, Phys. Rev. Lett. **79**, 4337 (1997).
- [10] R. Beck *et al.*, Phys. Rev. **C61**, 35204 (2000).
- [11] K. Batzner *et al.*, Nucl. Phys. **B76**, 1 (1974).
- [12] R. Siddle *et al.*, Nucl. Phys. **B35**, 93 (1971).
- [13] J. C. Alder *et al.*, Nucl. Phys. **B46**, 573 (1972).
- [14] F. Kalleicher *et al.*, Z. Phys. **A359**, 201 (1997).
- [15] V. V. Frolov *et al.*, Phys. Rev. Lett. **82**, 45 (1999).
- [16] C. N. Papanicolas, in *Topical Workshop on Excited Baryons*, World Scientific, Singapore, 1989; A.M. Bernstein *et al.*, Phys. Rev. **C47**, 1274 (1993).
- [17] D. Drechsel *et al.*, Nucl. Phys. **A645**, 145 (1999).
- [18] T. Sato and T.-S. H. Lee, Phys. Rev. **C54**, 2660 (1996).
- [19] R. M. Davidson *et al.*, Phys. Rev., **D43**, 71 (1991); R. M. Davidson and N. C. Mukhopadhyay, Phys. Lett. **B353**, 131 (1995).
- [20] R. L. Crawford, Nucl. Phys. **B28**, 573 (1971).
- [21] D. Drechsel and L. Tiator, J. Phys. G: Nucl. Part. Phys. **18**, 449 (1992).
- [22] G. A. Warren *et al.*, Phys. Rev. **C58**, 3722 (1998).
- [23] C. Mertz, PhD thesis, Arizona State University, unpublished (1998); C. Vellidis, PhD thesis, University of Athens, in preparation.
- [24] S. S. Kamalov, private communication, 2000.
- [25] T. Sato and T.-S. H. Lee, private communication, 2000, and to be published.
- [26] R. M. Davidson, private communication, 2000.

Model	$ M_{1+} $ ($10^{-3}/m_{\pi^+}$)	$\Re\epsilon(E_{1+}/M_{1+})$ (%)	$\Re\epsilon(S_{1+}/M_{1+})$ (%)	P_n
TME (a)	25.1 ± 0.7	0	-7.6 ± 0.8	—
TME (b)	24.5 ± 1.1	$+0.9 \pm 1.4$	-8.5 ± 1.2	—
RPI	25.4 ± 0.3	$+0.8 \pm 0.8$	-9.1 ± 0.8	-0.12
MAID	26.6 ± 0.2	-2.2 ± 0.2	-6.7 ± 0.2	-0.51
SL	27.7	-3.3	-4.3	-0.26

TABLE I. Multipoles extracted from the present data at $Q^2=0.126$ (GeV/c) 2 and $W=1232$ MeV. Statistical and systematic errors are added quadratically. The measured $P_n=-0.40 \pm 0.06$ at $W=1231$ MeV [22].

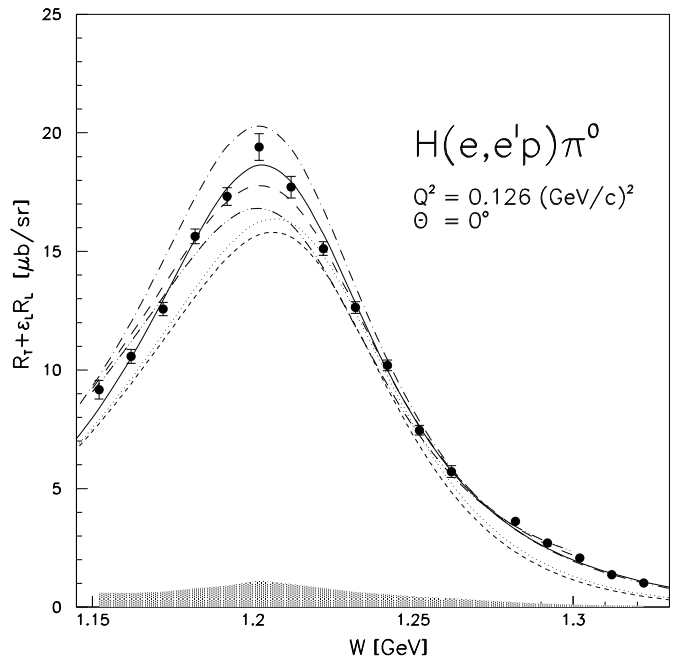


FIG. 1. The CM cross section in parallel kinematics. The solid curve is the fit of MAID [17,24] and the dot-dashed curve is the corresponding result for the resonant $E2=C2=0$. The long-dashed curve is the fit of RPI [19,26] and the dot-dot-dashed curve is the corresponding result for the resonant $C2=0$. The short-dashed and dotted curves are the “deformed” and “non-deformed” prediction of SL [18,25], respectively. The shaded band depicts the value of the systematic error.

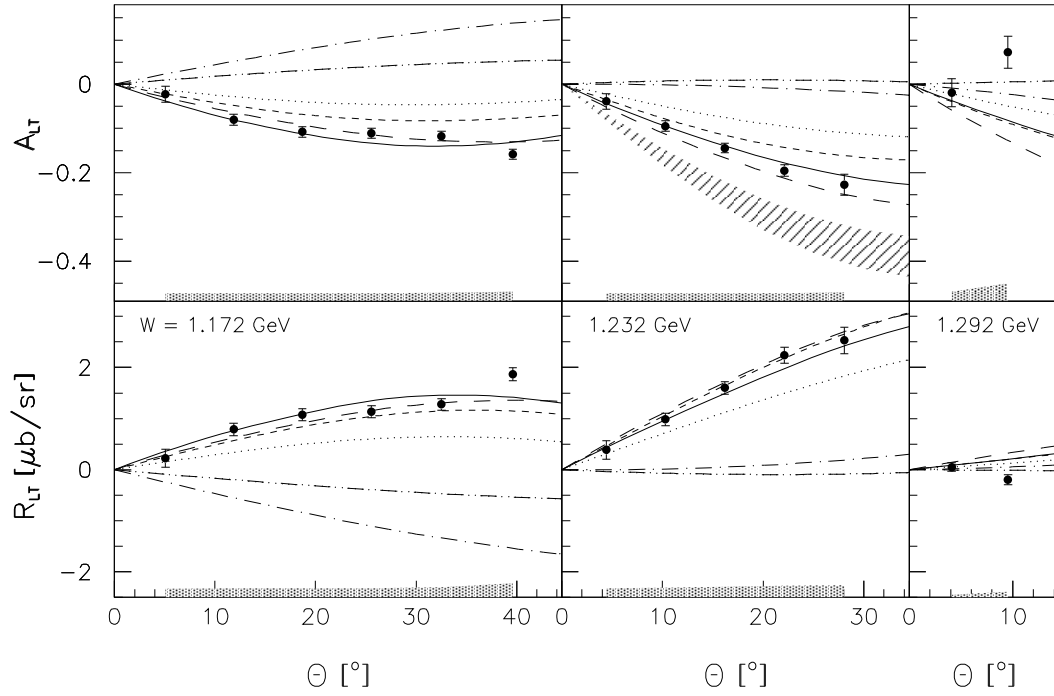


FIG. 2. The longitudinal-transverse asymmetry and response, as a function of the proton polar angle relative to \vec{q}_{cm} . The curves are explained in Fig. 1. The hatched band is the projection of the Bonn result [14], and the shaded bands depict the values of the systematic error.